*Inorganica Chimica Acta*, 75 (1983) 249–257



# Spectroscopic Studies of Metal Complexes Containing π-Delocalized Sulfur Ligands. The Resonance Raman Spectra of the Iron(II) and Iron(III) Complexes of the Antitumor Agent 2-Formylpyridin Thiosemicarbazone

HELOISA BERALDO* and LUCIA TOSI

*Département de Recherches Physiques, Université Pierre et Marie Curie, LA No. 71, 75230 Paris, Cédex 05, France*

Received April 1, 1983

*The resonance Raman spectra of the Fe(II) and Fe(III) complexes of 2-formylpyridine thiosemicarbazone have been measured in acid (pH 3.9–4.2) and alkaline (pH 7.4) aqueous media. In the spectra of both compounds the bands most strongly enhanced are due to skeletal modes (primarly CN and CS stretches) and ring deformations. On the basis of these results the strong visible absorption of these complexes is attributed to a pπ(S) → σ*(Fe) ligand to metal charge transfer transition. Moreover, the excitation profiles of the Fe(II) complex show a progression of peaks with regular spacing, which are interpteted as arising from successive vibrational levels involving the CS stretching mode. CN vibrations are very sensitive both to metal charge and protonation of the ligand whereas the CS vibrational frequencies are only dependent on metal charge. These results suggest appreciable dπ–dπ metal–sulfur back bonding in the Fe(II) complex.*

## Introduction

The α-(N-heterocyclic carboxaldehyde)thiosemicarbazones comprise a class of compounds possessing anti-neoplastic activity. These agents form very stable compounds with transition metal ions [1]. Several studies have shown that 2-formylpyridin thiosemicarbazone (FPT) and 1-formylisoquinoline thiosemicarbazone (IQ-1), the parent compounds of two of the most potent series, cause marked inhibition of DNA synthesis. The principal site of cellular reaction is ribonucleoside diphosphate reductase (RDR), an obligatory enzyme in the synthetic pathway of DNA precursors [2].

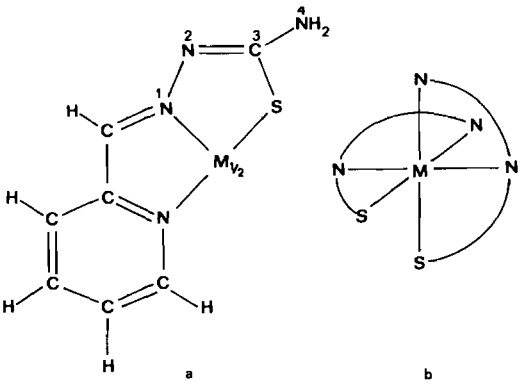

Fig. 1. General structure of a 2-formyl-pyridin thiosemicarbazone complex (a). Octahedral bichelate (b).

Both FPT and IQ-1 have in common the conjugate N⁻N⁻S tridentate ligating structure (Fig. 1a) which, as well as the need of a heterocyclic nitrogen, is a requisite for tumor inhibiting activity [1]. This tridentate ligand is able to form tetragonal 1:1 complexes with an oxygen of a water molecule in the fourth corner, square planar in the case of Cu(II) and tetrahedral in that of Zn(II), and 2:1 octahedral complexes in the case of Fe(II), Fe(III) and Ni(II); the structure of the Ni(II)(IQ-1)$_2$ complex has been determined and confirms these findings [3]. Two ligands are tridentately bound to the metal in two orthogonal planes (Fig. 1b).

Several results support the conclusion that the active form of the RDR inhibitor is the Fe(II) chelate. However, the mechanism of action is not clearly understood. The iron complex is particularly active against the mammalian RDR of some rodent tumors. The RDR of the rat Novikoff tumor that has been used for most *in vitro* tests consists of two protein units assumed to be non-identical and labelled

*On leave from the Department of Chemistry, Federal University of Minas Gerais, Belo Horizonte, Brazil.

0020-1693/83/$3.00

$P_1$ and $P_2$ [4]. In the RDR assay solution, Fe(II) or Fe(III) is always added to the medium, the latter being reduced to Fe(II) owing to the presence of dithiothreitol (DTT) which functions as the reducing substrate of the enzyme in the place of thioredoxin [2].

It appears that a more thorough investigation on the physicochemical properties of these compounds should give a more clear insight on their antitumor activity. As we have stated above, several derivatives of the parent compounds FPT and OQ-1 were synthesized and tested. Some physicochemical properties of Cu(II), Zn(II) and Fe(II) complexes of FPT and 5-substituted FPT have been studied by Petering and co-workers [5–7]. The Fe(II) complex of FPT in particular, is a 1:2 species with a large formation constant $\beta = 6.3 \times 10^{15}$. Its solubility in water is slightly higher than $10^{-4}$ *M* at pH 7. Its absorption spectrum displays a strong band around 610 nm ($\epsilon_M = 5900\ M^{-1}\ cm^{-1}$ l) with a shoulder at approximately 540 nm. These spectral characteristics make this complex particularly adapted to the study by means of resonance Raman (RR) spectroscopy.

The RR effect may be observed when the excitation frequency is tuned into the absorption band of a given chromophore. Under this condition the Raman intensity of those vibrations coupled with the corresponding electronic transition are enhanced by several orders of magnitude. RR spectroscopy is a powerful technique that provides structural and electronic information from complex molecules containing multiple chromophores.

In a previous report we have presented the results of an RR study on another complex containing a strongly delocalized thiosemicarbazone ring system and displaying antitumor activity, CuKTS [8]. In this paper we wish to report the results and conclusions of an RR investigation on the Fe(II) and Fe(III) complexes of FPT.

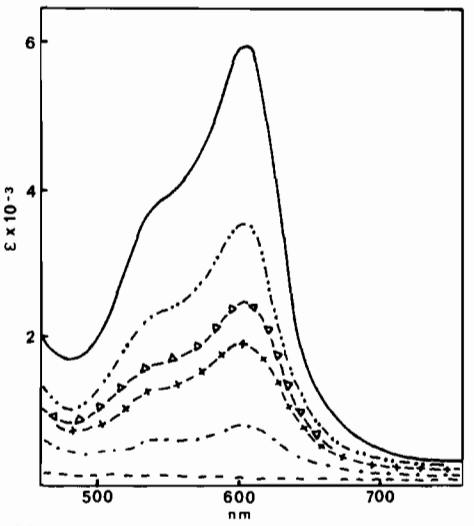


(a)

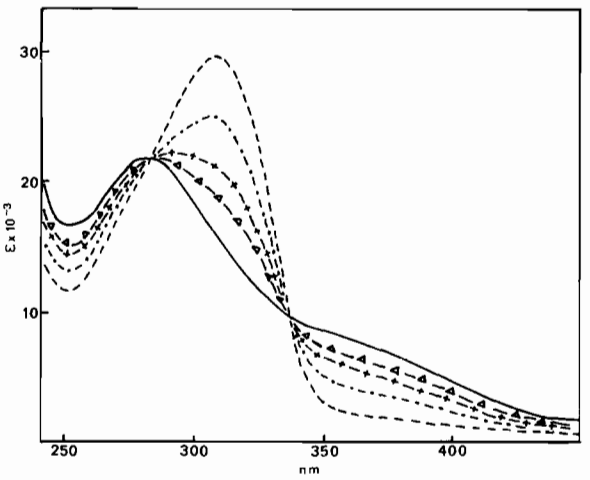


(b)

Fig. 2. Spectrophotometric titration curves of HFPT with Fe(II), Tris buffer pH 7.4 DTT 0.1 *M*. DMSO 1%. a) [Fe(II)]/[HFPT]: ------ 0; –·– 0.04; –+– 0.2; –△– 0.32; –··– 0.4; ——— 0.5. b) [Fe(II)]/[HFPT]: ------ 0; –·– 0.24; –+– 0.35; –△– 0.38; ——— 0.5. $\epsilon$ is expressed in terms of HFPT concentration.

## Experimental

2-formyl pyridin thiosemicarbazone (FPT) was obtained by the method of Anderson *et al.* [9]. The Fe(II) complex was prepared by the method of Ablov and Belichuk [10] and recrystallized from ethanol. All the other chemicals were of the best reagent grade. Demineralized distilled water, previously freed of organic contaminants, was used throughout.

Raman spectra were measured on a Coderg D 800 spectrometer equipped with holographic gratings. The detector used a DC amplifier and a cooled RCA C31034 PM tube. The exciting lines were those of $Ar^+$ and $Kr^+$ Spectra physics lasers and a Spectra Physics Rodamine 6G dye laser pumped by the $Ar^+$ laser. Raman intensities were measured relative to the intensity of the $\nu_1(ClO_4^-)$ band used as internal standard. The excitation profiles are reported as the ratio of the peak height of a given band to that of the internal standard. Intensity measurements using the area under the bands gave similar results. The ratios were corrected for sample absorption, instrumental spectral response and scattered radiation frequency.

Absorption measurements were made on a Cary 219 spectrometer. Unless stated otherwise, molar absorptivities are expressed in terms of Fe concentrations.

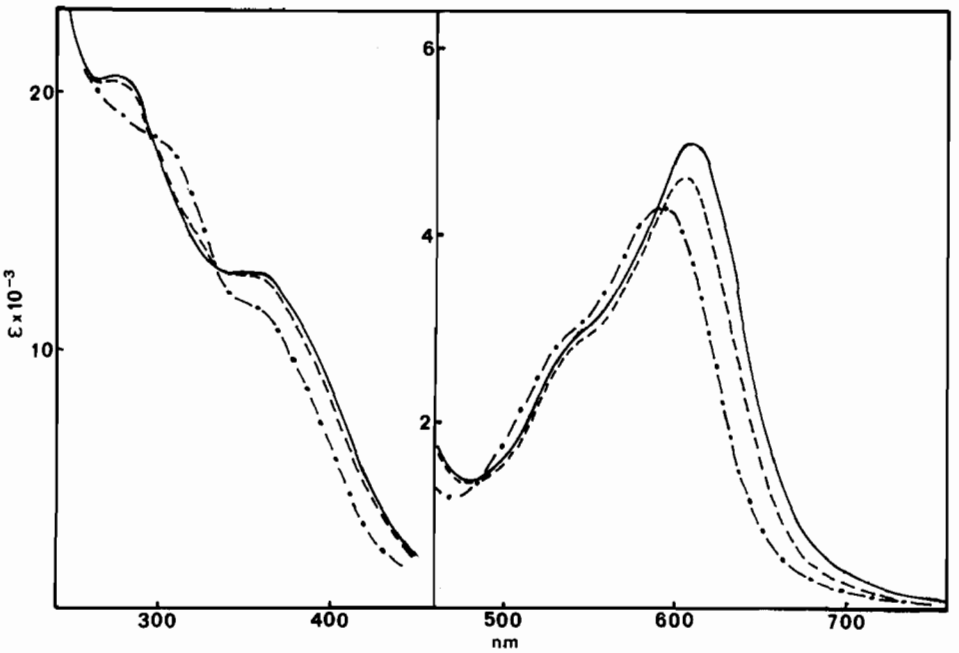


Fig. 3. Spectrophotometric acid–basic titration of Fe(II)$(FPT)_2$ in aqueous solution, DTT 0.1 *M*. –·– pH 4–4.5; ------ pH 5.6; —— pH 6.2 to 9.

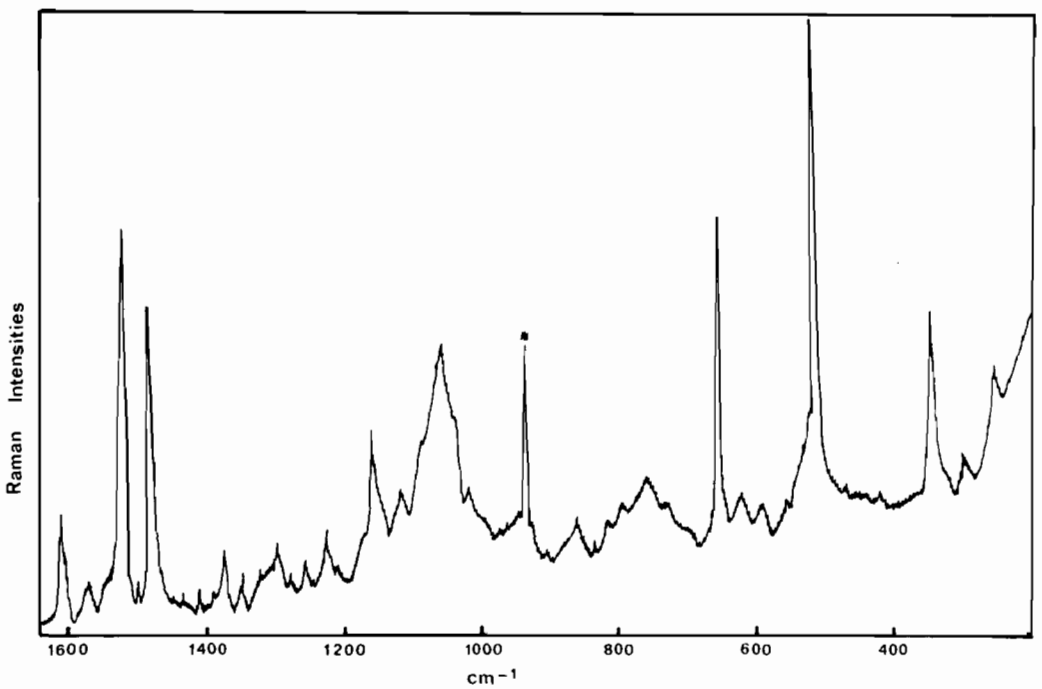


Fig. 4. Resonance Raman spectrum of Fe(II)$(FPT)_2$ $2.5 \times 10^{-4}$ *M*. Tris buffer pH 7.4, DTT 0.1 *M*, $ClO_4^-$ 0.05 *M*, using the 595.3 nm Rodamine 6G excitation line, 150 mw, slit width 5 $cm^{-1}$, scanning speed 25 $cm^{-1}$/min, time constant 0.5 sec. The asterisk indicates the $\nu_1$ $ClO_4^-$ band.

## Results

The titration curves of HFPT with Fe(II) at pH 7.4, Tris buffer DMSO 1% in the presence of DTT are illustrated in Fig. 2 (a and b). The absorption spectrum of the ligand displays a strong band at 315 nm (31750 $cm^{-1}$; $\epsilon = 29500\ M^{-1}\ cm^{-1}$ l). The absorption spectrum of Fe(II)$(FPT)_2$, on the other hand,

TABLE I. Resonance Raman Frequencies and Assignments.

| Fe(II)(FPT)$_2$ | | | Fe(III)(FPT)$_2$ | Assignments |
|---|---|---|---|---|
| $H_2O$ | | $D_2O$ | $H_2O$ | |
| pH 7.4 | pH 4.0 | pD 4.2 | pH 3.9 or 7.4 | |
| 1605m | 1607m | 1610m | 1612m | $\nu_{CC}$ pyridin |
| 1561vw | 1568w | – | 1577vw | |
| 1522s | 1533s | 1540s | 1550vs | |
| 1480s | 1472s | 1475s | 1495w | mainly $\nu_{CN} + \nu_{CC}$ |
| – | – | – | 1465m | |
| – | – | – | 1443m | |
| 1375w | 1375w | 1385w | – | |
| 1350w | – | 1320w | 1330vw | |
| 1295vw | 1295w | 1295vw | 1300vw | mainly $\nu_{CN} + \nu_{NN}$ |
| 1252vw | 1257vw | – | 1262vw | not enhanced |
| 1223w | 1225w | 1226m | 1233m | |
| 1157m | 1157m | 1162m | 1162w | |
| 1115w | 1116w | 1125w | 1120vw | |
| 1060m | 1070w | 1067w | – | $\nu_{NN} + \nu_{CN}$ |
| 1022w | 1022w | 1022m | 1030m | |
| 860vw | 890vw | – | – | 512 + 345 |
| 805vw | – | – | – | |
| 790w | 788vw | – | – | DTT |
| 758w | 748vw | – | – | |
| 733w | – | – | 725vw | |
| 695w | – | – | 695vw | ring deformation |
| 655s | 655s | 655s | 655vw | ring deformation |
| 622vw | 625vw | 617vw | 626m | ring deformation |
| 590vw | 595w | 593vw | – | ring deformation |
| – | – | – | 527m | $\nu_{CS}$ |
| 512vs | 515vs | 505vs | 515 m | $\nu_{CS}$ |
| – | 458vw | – | 455w | $\nu_{MN}$ |
| – | 412vw | – | 422vw | $\nu_{MN}$ |
| 345m | 348m | 340m | 362vw | $\nu_{CS} + \nu_{MS}$ |
| – | – | – | 312vw | $\nu_{MS}$ |
| 250vw | – | 258vw | – | $\nu_{MS}$ |

presents one band at 607 nm (16470 $cm^{-1}$; $\epsilon$ = 5900 $M^{-1}$ $cm^{-1}$ l) with a shoulder at 540 nm (18500 $cm^{-1}$: $\epsilon$ = 3200 $M^{-1}$ $cm^{-1}$ l). The ligand band is split in two others at 360 nm (27800 $cm^{-1}$: $\epsilon$ = 16300) and at 280 nm (35700 $cm^{-1}$; $\epsilon$ = 46200). When the complex Fe(II)(FPT)$_2$ is dissolved in water the absorption spectrum remains practically unchanged from pH 6.2 to 10, although some dissociation takes place at high pH as the decrease of absorption at 607 and 540 nm indicates. Below pH 6.2 and down to pH 4.5 the band at 607 nm and the shoulder at 540 nm shift to higher frequencies, at 586 and 506 nm respectively; concomitantly, the band at 280 shifts to 310 nm whereas the shoulder at 360 remains unaltered, both bands decreasing in intensity (Fig. 3). Three isosbestic points at 484, 330 and 292 nm indicate the presence of two species. Below pH 4 the intensity of all bands decreases whereas that at 310 nm increases, indicating dissociation.

A characteristic RR spectrum of Fe(II)(FPT)$_2$ at pH 7.4 upon excitation into the visible absorption envelope is shown in Fig. 4. The vibrational assignments are summarized in Table I. At first glance this spectrum appears remarkably similar to that of CuKTS [8]. However, some differences are noticeable. There is a limited number of strong bands which are resonance enhanced. The excitation profiles are obtained by plotting the corrected Raman intensities against the laser excitation frequencies. They are illustrated in Figs. 5 and 6 together with the absorption spectrum.

Of the group of bands lying above 1000 $cm^{-1}$ (Fig. 5), the most intense and strongly enhanced lie at 1525 and 1480 $cm^{-1}$. Two similar bands at 1537 and 1460 $cm^{-1}$ observed in the RR spectra of CuKTS were assigned by us to skeletal vibrations, mainly the stretching mode of the conjugated delocalized double bonded C=N of the trichelate ring [8]. We

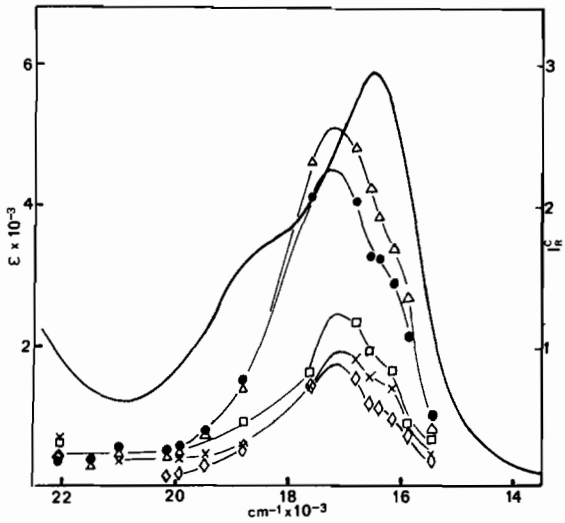


Fig. 5. Raman excitation profiles of Fe(II)(FPT)$_2$ in Tris buffer pH 7.4, DTT 0.1 *M*. —— absorption spectrum, $I_R^c$ are the corrected intensity ratios in arbitrary units. Raman bands (△) 1515 cm$^{-1}$; (●) 1480 cm$^{-1}$; (□) 1060 cm$^{-1}$; (×) 1022 ≅ 1157 cm$^{-1}$; (◇) 1605 cm$^{-1}$.

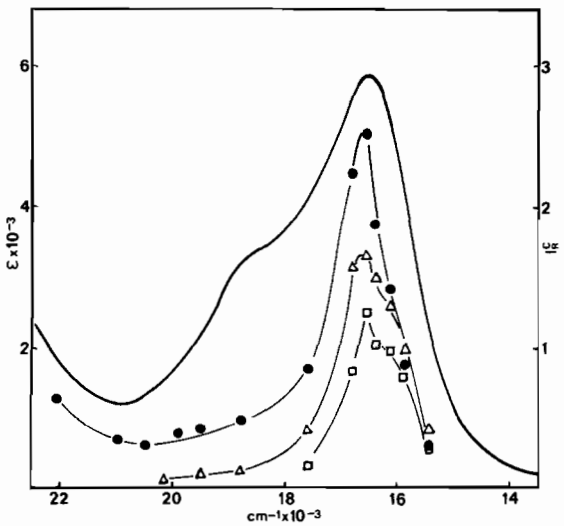


Fig. 6. Raman excitation profile of Fe(II)(FPT)$_2$ in Tris buffer pH 7.4, DTT 0.1 *M*. —— absorption spectrum, $I_R^c$ as in Fig. 5. Raman bands: (△) 655 cm$^{-1}$; (○) 512 cm$^{-1}$; (□) 345 cm$^{-1}$.

propose a similar assignment for the bichelate ring of Fe(II)(FPT)$_2$.

The Raman spectrum of pyridin displays a weak band at 1480 cm$^{-1}$ assigned to the 19a skeletal vibration of the monosubstituted benzene ring, and a medium doublet at 1590–1600 cm$^{-1}$ assigned to the 8a skeletal mode [11]. Some contribution of both vibrations in the RR spectra of Fe(II)(FPT)$_2$ cannot be discarded as some delocalization into the pyridine ring seems plausible. However, taking into account the strong similarity between the RR spectra of CuKTS and Fe(II)(FPT)$_2$ in this region, the contribution, if present, must be small. We therefore propose to assign the medium band at 1605 cm$^{-1}$, only slightly enhanced to the CC skeletal mode of pyridin. The medium band at 1157 and the weaker one at 1115 cm$^{-1}$ may also be attributed to skeletal stretches coupled with C=N modes, especially the NN stretching vibrations.

As the excitation frequency approaches an electronic transition the Raman bands whose intensity is enhanced are precisely those corresponding to the vibrations coupled with that particular electronic transition. As illustrated by Fig. 5 all the Raman modes described above are coupled with one electronic transition lying around 580 nm (17150 cm$^{-1}$) and another one at 620 nm (16.200 cm$^{-1}$).

From the group of bands lying below 1000 cm$^{-1}$ (Fig. 6) the most strongly enhanced are those at 655, 512 and 345 cm$^{-1}$, the corresponding vibrational modes being coupled with one electronic transition at 600 nm (16,600 cm$^{-1}$) and another one at about 620 nm (16,200 cm$^{-1}$). The intensity increase at 512 cm$^{-1}$ is by far the strongest, approximately 9 times the values observed far from resonance. The 512 cm$^{-1}$ band appears also to be in resonance with one of the ultraviolet ligand bands.

We propose to assign the band at 512 cm$^{-1}$ mainly to the CS stretching vibration. It has been shown that the CS stretch is distributed among three strong bands in the vibrational spectra of thiosemicarbazide (TSC). These bands lie at 1010, 808 and 508 cm$^{-1}$ in the Raman spectrum. The bands at 808 cm$^{-1}$, which shifts markedly upon complexation (~100 cm$^{-1}$) arises from a pure CS stretch while the N(4)H$_2$ rocking mode contributes to the peak at 1010 cm$^{-1}$, and the NCN deformation to that at 508 cm$^{-1}$ [12]. If our assignment is correct the shift of 300 cm$^{-1}$ of the CS stretch is quite impressive and is, as far as we know, the first example of such a strong effect upon coordination. The bands at 655 and 345 cm$^{-1}$, which are less enhanced, may be assigned to ring deformation coupled with the CS stretch. The MS stretch however may also be associated to the band at 345 cm$^{-1}$, since this frequency is quite reasonable for a metal–ligand stretching mode [13, 14]. We have observed a rather analogous pattern in the RR spectra of CuKTS, although here the strongest and most enhanced band lies at 714 cm$^{-1}$. The very weak bands at 860 and 805 cm$^{-1}$ are probably combinations (512 + 345; 655 + 250) whereas those at 790, 758 and 733 are due to DTT.

Some comments must be made regarding the strong and broad band at 1060 cm$^{-1}$ observed at pH 7.4 over which are superimposed two weak peaks at 1022 and 1122 cm$^{-1}$ (see Fig. 4). The whole broad feature appears to be in resonance with the band at 17100 cm$^{-1}$. At pH 3.9 however the

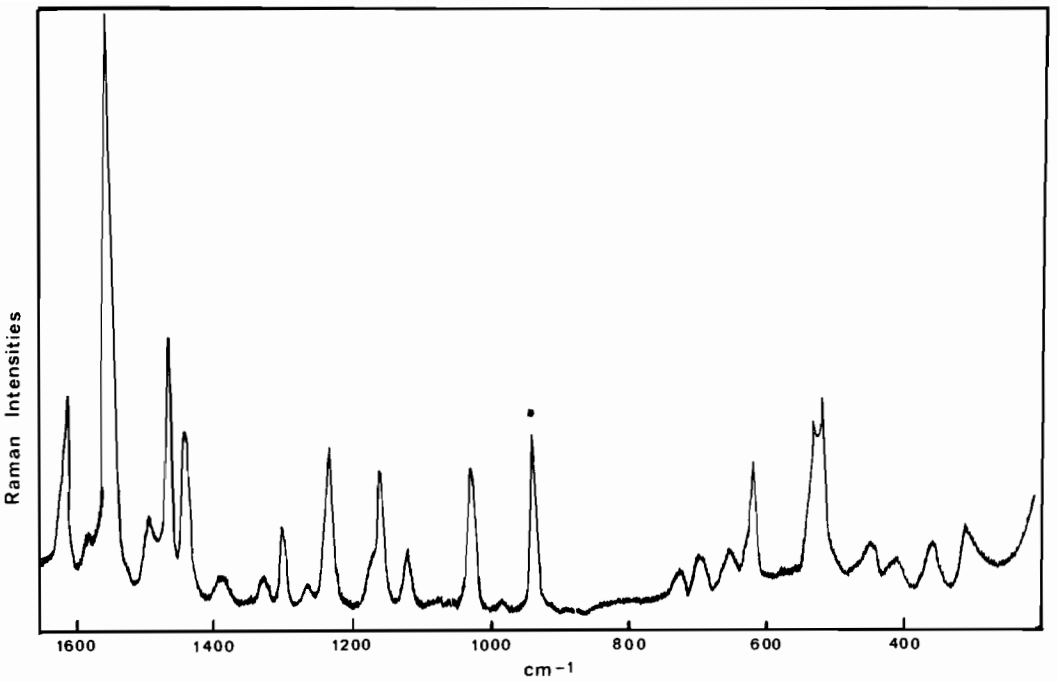


Fig. 7. Resonance Raman spectrum of Fe(III)(FPT)$_2$ 5 × $10^{-4}$ *M*, Tris buffer pH 7.4, $ClO_4^-$ 0.05 *M*, using the 457.9 nm $Ar^+$ excitation line, 100 mW, slit width 5 $cm^{-1}$, scanning speed 50 $cm^{-1}$/min, time constant 0.5 sec. The asterisk indicates the $\nu_1$ $ClO_4^-$ band.

RR spectra show three weak bands at 1022, 1070 and 1116 $cm^{-1}$ that are not appreciably enhanced. The band at 1060 $cm^{-1}$ in the spectrum of Fig. 4 is too broad to be ascribed to a vibrational mode of the complex. It is strongly polarized and lies approximately at the same frequency as one of the bands of the sample holder attributed to the SiO stretching mode of non-bridged silicate [15]. We have observed a similar feature in the spectra of CuKTS that appeared to be in resonance with an UV transition, and ascribed this behavior to an interaction of the silicate ions of the sample holder with the complex, taking place at pH $\geqslant$ 7 [8]. Although in the present case the band is in resonance with one visible electronic transition, we propose the same origin on the basis of the polarization ratio ($\rho \cong 0$) as compared with that of the other Raman bands ($\rho = 0.3$–0.6).

As we have stated above, the curves of Fig. 3 demonstrate the presence of two species in equilibrium, the one at low pH containing the protonated form of the ligand: HFPT [10]. This protonation must take place at N(2). The RR spectra of Fe(II)-$(HFPT)_2^{2+}$ obtained at pH 4–4.2 when the protonation is completed are very similar to those of the deprotonated form, although the band intensities decrease somewhat, particularly below 1000 $cm^{-1}$. However changes in band frequencies are noticeable in the CN stretching region. The bands at 1480 $cm^{-1}$ and 1522 $cm^{-1}$ shift to 1472 and 1533 $cm^{-1}$ respectively, increasing the gap between them from 42 $cm^{-1}$ at pH 7.4 to 61 $cm^{-1}$ at pH 3.9. There are also some other very slight shifts (see Table I).

The RR spectra of the Fe(II) complex in $D_2O$ solution, where the N(2) and N(4) hydrogens of TSC are replaced by deuterium, give additional support to our assignments (see Table I). The spectra of the deuterated form correspond to those of the protonated form of the complex (pD = 4.2) and are analogous to those observed in water at pH 4. If one excepts the weak band at 1568 $cm^{-1}$ that apparently shifts to lower frequencies, the frequencies of the other bands lying above 1000 $cm^{-1}$ remain practically unchanged, with a tendency in the skeletal modes to shift to higher frequencies. This result corroborates our assumption that all these peaks are due to the ring skeletal modes with no contribution of the exocyclic vibrations, namely $N(4)H_2$ or N(2)H deformations. In the region below 1000 $cm^{-1}$, on the other hand, small but significant shifts to lower frequencies can be detected in two bands: at 515 to 505 $cm^{-1}$ and 348 to 340 $cm^{-1}$. As has been pointed out the CS mode is expected to shift slightly upon deuteration at N(4) [12]. So, both bands must contain contributions of the CS stretch, in particular the 515 $cm^{-1}$ one which must be ascribed unambiguously to the CS vibration.

Finally the weak bands at 458, 412 $cm^{-1}$ in the

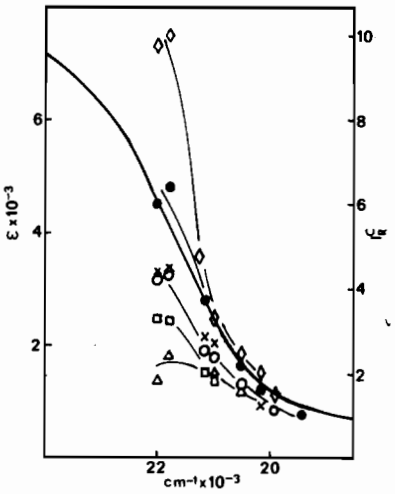


Fig. 8. Raman excitation profiles of the Fe(III) complex of FPT, Tris buffer pH 7.4 —— absorption spectrum $I_R{}^c$ has the same meaning of Fig. 5. Raman bands: (●) 1550 $cm^{-1}$; (○) 1465–1445 $cm^{-1}$; (×) 1161 $cm^{-1}$ ≅ 1028 $cm^{-1}$; (◇) 527–515 $cm^{-1}$; (□) 626 $cm^{-1}$; (△) 362 $cm^{-1}$.

RR spectra of the protonated (deuterated) form are tentatively assigned to the FeN stretches whereas those below 300 $cm^{-1}$ to FeS stretches and FeSC deformation modes [14].

Upon exposure to air, an aqueous solution of $Fe(II)(FPT)_2$ slowly oxidizes to the Fe(III) form of the complex, which is the thermodynamically stable form in this medium. The absorption at 607 nm moves to higher frequencies and appears as a shoulder at 435 nm (23000 $cm^{-1}$, $\epsilon$ = 6000 $M^{-1}$ $cm^{-1}$ l) [5]. The two strong bands in the UV region shift to 340 nm (29400 $cm^{-1}$) and 310 nm (32100 $cm^{-1}$). Isosbestic points are observed at 492 and 370 nm, consistent with the presence of two interconverting species. The absorption spectra of this species at pH 3.9 and 7.4 are strictly analogous.

A typical RR spectrum of the Fe(III) complex is presented in Fig. 7. In Table I are reported the corresponding frequencies and assignments. The excitation profiles are presented in Fig. 8. To facilitate comparison the Raman intensities have been scaled to unity at 514.5 nm (19436 $cm^{-1}$). Since in this case we are working in pre-resonance conditions, all the Raman modes appear to be more or less coupled with one electronic transition at ~460 nm (~21800 $cm^{-1}$). Several spectral changes in relative intensity and in frequencies are noticeable in going from the Fe(II) to the Fe(III) complex. In particular the band at 1522 $cm^{-1}$ shifts to 1550 $cm^{-1}$, whereas that at 1480 $cm^{-1}$ moves to lower frequencies and splits in two others of medium intensity at 1465 and 1443 $cm^{-1}$. The band at 1550 $cm^{-1}$ is by far the most intense and is strongly enhanced (~6 times). The region between 1300 and 1000 $cm^{-1}$ is not appreciably affected and the band intensities are increased 3 or 4 times.

In the CS stretching region the bands are considerably weaker. Although the intensity measurements are less accurate in this region, the most strongly enhanced of the overall spectrum is the doublet at 528–515 $cm^{-1}$, the intensity of which increases approximately 10 times. The weak peak at 622 $cm^{-1}$ of the Fe(II) complex spectrum shifts to 626 $cm^{-1}$ and shows moderate resonance enhancement. The other bands are even weaker and enhanced to a lesser degree. Strictly analogous spectra are obtained at pH 3.9.

## Discussion

$Fe(II)(FPT)_2$ is an EPR-silent complex which yields upon oxidation the Fe(III) low spin species (g = 2.185, 2.140, 2.000). As has been shown the protonated and deprotonated forms of the Fe(II) complex are also in the low spin state [10]: the $d\pi$ orbitals of the Fe(II) complex are filled. There is one half-filled $d\pi$ orbital in the Fe(III) complex and two vacant antibonding orbitals in both complexes. The existence of the metal half-filled or vacant orbitals, as well as that of three lone pairs in thiolate may, in principle, result in three ligand-to-metal-charge-transfer (LMCT) transtions in the spectra of both complexes: one $\sigma(S) \rightarrow \sigma^*(Fe)$ of higher energy and two $p\pi(S) \rightarrow \sigma^*(Fe)$ (or $p\pi(S) \rightarrow d\pi(Fe)$ in the case of Fe(III)) of lower frequency.

As pointed out by Hirakawa and Tsuboi [16], the enhancement of a Raman band at resonance is an indication that the equilibrium conformation of the molecule is distorted along the corresponding normal coordinate in the excited electronic state. If the electronic transition involves a $p\pi(S) \rightarrow$ Fe(II) LMCT, one of the lone pair electrons on the sulfur should be brought onto the antibonding orbital of the metal during the transition. In such circumstances the C–S bond length is expected to become longer in the excited state. Besides, the depopulation of the sulfur orbital should lower the extent of conjugation with the $\pi$ system of the bichelate ring, which is assumed to be highly delocalized [1]. The vibrations predominantly coupled with the LMCT transition should accordingly be the CS and ring skeletal modes, and possibly ring deformations coupled with them. As we have shown above these are precisely the bands most strongly enhanced in the spectra of $Fe(II)(FPT)_2$, $Fe(II)(HFPT)_2^{+2}$ and the Fe(III) complex. Moreover, if the charge transfer arises from a $\pi$ donor orbital the metal–ligand bond length should not be strongly altered during the transition. Hence, the metal–ligand bands should be

moderately enhanced, and this also is what one observes in the excitation profiles of Figs. 5, 6 and 8.

These spectral features give good grounds for the assignments of the electronic bands to which these vibrations are coupled to the $p\pi(S)-\sigma^*Fe(II)$ and $p\pi(S)-\sigma^*Fe(III)$ LMCT transitions. As has been seen before, the excitation profiles of the $Fe(II)(FPT)_2$ show different enhancement pattern for the Raman peaks lying above or below 1000 $cm^{-1}$. The former are in resonance with two electronic transitions at ~16200 and ~17150 $cm^{-1}$. The latter with two electronic transitions at ~16200 and ~16600 $cm^{-1}$. This excitation pattern with peak spacing of approximately 400–450 $cm^{-1}$ strongly suggests a resonance Raman scattering from a series of excited vibrational levels, as has been observed in the case of the RR spectra of Fe(III)–transferrin [17]. As stated above, the C–S bond is expected to increase appreciably in the excited state owing to depopulation of the sulfur $p\pi$ orbital. This should be the major structural change during the transition so that a Franck–Condon progression in the CS stretching vibration is quite plausible. As a consequence of the lengthening in the CS bond a significant decrease from the ground state $\nu_{CS}$ frequency value (512 $cm^{-1}$) should then be expected. A value of 400–450 $cm^{-1}$ appears to be reasonable.

We thus assign the first maximum of the excitation profile of Figs. 5 and 6, at approximately 16200 $cm^{-1}$, to the origin (0–0) of the $p\pi(S)-\sigma^*$(Fe(II) electronic transition. The other maxima correspond to the (0–1) and (0–2) transitions to vibrational levels involving the CS stretch. Although there is a gap in our laser in the region comprised between the (O–2) and (O–3) transitions, the sudden decrease in intensity of the Raman peaks at 512, 655 and 345 $cm^{-1}$ precludes the presence of another maximum in this region. This also seems to be the case for the bands above and below 1000 $cm^{-1}$, between the (0–3) and the (0–4) transitions. Other vibrations associated with structural changes in the excited state may show much weaker Franck–Condon progressions, which are undetected. They may give rise to the smooth pattern observed between the first and third maximum in the excitation profiles of the Raman bands above 1000 $cm^{-1}$, probably masking the second maximum.

We have observed a similar pattern in the excitation profile of CuKTS [8] which exhibited Raman bands in resonance with two electronic transitions lying 1900 $cm^{-1}$ apart. We have then assigned both electronic bands to the two $p\pi(S) \rightarrow \sigma^*Cu(II)$ LMCT transitions, although we did not discard the possibility of a vibrational progression. We think at present that the second hypothesis is more plausible.

The changes in vibrational frequencies reflect the distortions occurring in the ground state. Since in the protonated form of the Fe(II) complex at N(2) the ligand contains a thiono sulfur one must expect an increase in the double bond character of the CS bond and a lesser conjugation of the double bonded C=N. The shifting of the CN stretching frequencies appears to confirm these assumptions. Strikingly, the CS stretching mode seems to be practically insensitive to protonation (*cf.* CuKTS, where protonation of the ligand at N(2) causes a strong shift of the CS mode to higher frequencies [8]). One must recall, however, that thiono and thiolate sulfurs possess vacant $d\pi$ orbitals which can be used for $d\pi-d\pi$ metal–sulfur bonding. Although thiono sulfur is less polarizable than thiolate sulfur it may be a better $d\pi$ electron acceptor than thiolate sulfur [18]. In addition, low spin Fe(II) is known for its tendency to $d\pi$ electron back donation. Back electron transfer to a $d\pi$ sulfur orbital should diminish the order of the CS bond resulting in compensating effects that lead ultimately to the observed invariance in the CS stretch.

As was remarked before, the RR spectra of the Fe(III) complex is strictly analogous at pH 3.9 or 7. It is difficult to ascertain in this case which of the forms is under study: protonated or deprotonated. However, taking into account that Fe(III) has a much lesser ability than Fe(II) for back bonding donation one must expect a higher CS stretching frequency in the spectrum of the protonated Fe(III) complex. One observes, in fact, a splitting of the CS vibration with a moderate shifting of the mid point to higher frequencies of the order of 9 $cm^{-1}$. It is interesting to note, in addition, that from the two UV bands in the Fe(II) complex absorption spectrum it is only the high energy one (at 280 nm) which is sensitive to protonation, shifting to lower frequencies (310 nm). The low energy band (at 360 nm) on the other hand, seems to be sensitive, although to a lesser extent, to the charge of the metal shifting to higher frequencies (340 nm) passing from Fe(II) to Fe(III). All these observations suggest that in Fe(III) complex the ligand is protonated. In any case, it is clear that the metal charge induces shifts and splittings in the ligand vibrational frequencies, in particular in the CN and CS stretching regions and that the source of these shifts may be accounted for by a decrease in back bonding donation. There is also some effect in Raman intensities, but the origin of this effect is not clear.

The first important conclusion to be drawn from these results is that the bichelate is a strongly delocalized system and that the electronic spectrum of the Fe(II) complex is dominated by a low energy $p\pi(S) \rightarrow \sigma^*M$ LMCT transition. This would explain, in part, as stated by French and Blanz [19], the reactivity of this type of complex.

The second important conclusion concerns the ability of the Fe(II) complex to remove protons from

the medium in a short range of pH, without changing appreciably the energy of the transition and the extent of the back bonding. All this should facilitate the involvement of the Fe(II) complex as a system capable of draining protons from a given medium and able to inhibit any reaction strongly dependent of proton supply in a limited range of pH, namely, 4.5 to 6.2.

## Acknowledgements

H.B. Is indebted to CAPES from Brazil for a fellowship.

Technical assistance by L. Leroy is acknowledged.

## References

1 F. A. French and E. J. Blanz, Jr., *Cancer. Res., 25,* 1454 (1965).
*ibid., 26,* 1638 (1966).
2 A. C. Sartorelli, K. C. Agrawal, A. S. Tsiftsoglou and E. C. Moore, in 'Advances in Enzyme Regulation', G. Weber, ed., Pergamon Press, N. York, vol. 15, 117 (1977).
3 M. Mathew and G. J. Palenik, *J. Am. Chem. Soc., 19,* 6310 (1969).
4 E. C. Moore, in 'Advances in Enzymes Regulation', G. Weber, ed., Pergamon Press, N. York, vol. 15, 101 (1977).
5 W. Antholine, J. Knight, H. Whelan and D. H. Petering, *Mol. Pharmacol., 13,* 89 (1977).
6 W. E. Antholine, J. M. Knight and D. H. Petering, *Inorg. Chem., 16,* 569 (1977).
7 J. M. Knight, H. Whelan and D. H. Petering, *J. Inorg. Biochem., 11,* 327 (1979).
8 L. Tosi and A. Garnier-Suillerot, *J. Chem. Soc. Dalton Trans.,* 103 (1982).
9 F. L. Anderson, C. J. Duca and J. V. Scudi, *J. Am. Chem. Soc., 73,* 4967 (1951).
10 A. V. Ablov and N. I Belichuk, *Russ. J. Inorg. Chem., 14,* 93 (1969).
11 L. Corrsin, B. J. Fax and R. C. Lord, *J. Chem. Phys., 21,* 1170 (1953).
12 G. Keretszury and M. P. Marzocchi, *Spectrochim. Acta, 31A,* 275 (1975).
13 M. C. Jain, R. K. Sharma and P. C. Jain, *J. Inorg. Nucl. Chem., 42,* 1229 (1980).
14 D. P. Strommen, K. Bajdor, R. S. Czernuszewicz, E. L. Blinn and K. Nakamoto, *Inorg. Chim. Acta, 63,* 151 (1982).
15 M. Hass, *J. Phys. Chem. Solids, 31,* 415 (1970).
16 A. Y. Hirakawa and M. Tsuboi, *Science, 188,* 359 (1975).
17 B. P. Gaber, V. Miskowski and T. G. Spiro, *J. Am. Chem. Soc., 96,* 6868 (1974).
18 M. Akbar Ali and S. E. Livingstone, *Coord. Chem. Rev., 13,* 101 (1974).
19 F. A. French and E. J. Blanz, Jr., *J. Med. Chem., 9,* 585 (1966).